Chapter 7

Secondary Organic Aerosol Formation from the Ozonolysis of Cycloalkenes and Related Compounds*

* This chapter is reproduced by permission from "Secondary organic aerosol formation from ozonolysis of cycloalkenes and related compounds" by M.D. Keywood, V. Varutbangkul, R. Bahreini, R.C. Flagan, J.H. Seinfeld, *Environmental Science and Technology*, 38 (15): 4157-4164, 2004.

7.1. Abstract

The secondary organic aerosol (SOA) yields from the laboratory chamber ozonolysis of a series of cycloalkenes and related compounds are reported. The aim of this work is to investigate the effect of the structure of the hydrocarbon parent molecule on SOA formation for a homologous set of compounds. Aspects of the compound structures that are varied include the number of carbon atoms present in the cycloalkene ring (C_5 to C_8), the presence and location of methyl groups, and the presence of an exocyclic or endocyclic double bond. The specific compounds considered here are cyclopentene, cyclohexene, cycloheptene, cyclooctene, 1-methyl-1-cyclopentene, 1-methyl-1-cyclohexene, 1-methyl-1-cycloheptene, 3-methyl-1-cyclohexene, and methylene cyclohexane. SOA yield is found to be a function of the number of carbons present in the cycloalkene ring, with increasing number resulting in increased yield. Yield is enhanced by the presence of a methyl group located at a double-bonded site but reduced by the presence of a methyl group at a non-double bonded site. The presence of an exocyclic double bond also leads to a reduced yield relative to the equivalent methylated cycloalkene. On the basis of these observations, the SOA yield for terpinolene relative to the other cyclic alkenes is qualitatively predicted, and this prediction compares well to measurements of SOA yield from the ozonolysis of terpinolene. This work shows that relative SOA yields from ozonolysis of cyclic alkenes can be qualitatively predicted from properties of the parent hydrocarbons.

7.2. Introduction

Secondary organic aerosol (SOA) is ubiquitous in the atmosphere, being present in both urban and remote locations (1-2). SOA is formed when a parent volatile organic

compound is oxidized to form products with sufficiently low vapor pressures so that the products undergo absorptive partitioning between the gas and particle phase (3). In the atmosphere, parent hydrocarbons are both natural and anthropogenic in origin. Recently, a large number of compounds with strong potential for SOA formation, such as long chain alkenes and high molecular weight oxygenated hydrocarbons, have been identified in the urban atmosphere (4). In the remote atmosphere, SOA precursor hydrocarbons are predominately biogenic in origin and include the monoterpenes, α-pinene and β-pinene, and sesquiterpenes such as α-humulene and β-caryophyllene (5).

The formation of SOA from parent organics is studied in laboratory chambers e.g. Cocker et al. (6). Information obtained from SOA chamber experiments includes the chemical composition of products formed and the amount of SOA produced from a particular concentration of precursor hydrocarbon. Aerosol yield is a measure of the aerosol forming potential of a parent hydrocarbon (7-8), where yield (Y) can be defined as the ratio of organic aerosol mass concentration produced (ΔM_o, μg m^{-3}) to the mass concentration of hydrocarbon consumed (ΔHC, μg m^{-3}), $Y = \Delta M_o / \Delta HC$.

During the gas-phase oxidation of the parent hydrocarbon, semi-volatile organic gases are produced, which condense onto an existing particle phase once the product exceeds a saturation concentration. The experimentally measured aerosol yield, resulting from the oxidation of a single parent hydrocarbon has been correlated empirically, as resulting from absorptive partitioning of two semi-volatile products for over 40 parent hydrocarbons (7-8),

$$Y = \Delta M_o \sum_{i=1}^{2} \frac{\alpha_i K_{om,i}}{1 + K_{om,i} \Delta M_o} \qquad (1)$$

where α_i is the mass-based gas-phase stochiometric fraction for species *i*, and $K_{om,i}$ is the partitioning coefficient for species *i*. In effect, one product represents more volatile compounds and the second product represents products with lower volatility. Atmospheric models have been developed that include prediction of SOA production, including treatment of absorptive partitioning (9-11). Measurements from chamber experiments provide the fundamental data required to test the prediction of aerosol formation from first principles.

The ultimate aim of the current investigation is to understand how the structure of a precursor hydrocarbon influences the formation of SOA and to use this information to predict the SOA formation potential of compounds for which yield data do not exist. The system of cycloalkenes was chosen for its simplicity relative to atmospherically relevant SOA precursors such as the biogenic monoterpenes and sesquiterpenes. Cycloalkenes may be viewed, in a sense, as the simplified structures on which these more complicated compounds are based. In addition, the cyclohexene-ozone system itself has been extensively investigated, so that the gas and aerosol phase products have been relatively well-characterized (12-14). Ozonolysis of the cycloalkenes has been previously studied from the point of view of the gas-phase mechanism of oxidation (15; 19-24), the yield of SOA (12; 13), and identification of the aerosol products formed (13; 16-18; 21; 24-26).

We report here on a series of chamber experiments carried out in the Caltech Indoor Chamber Facility, in which SOA yields were measured in the ozonolysis of cycloalkenes and related compounds (Figure 7.1). Properties of the precursor cycloalkenes varied include the number of carbons within the ring (C_5 to C_8), the presence of methyl groups,

the presence of an exocyclic double bond, and the location of the methyl group relative to the endocyclic double bond.

Until very recently, molecular speciation analysis of laboratory and ambient SOA indicated that oxidation of both anthropogenic (aromatic) and biogenic (e.g., terpenes) parent organics leads to the formation of oxygenated monomeric compounds (12; 28-30) and some dimers (31). It is well established that the reaction between cyclohexene and ozone is initiated by the addition of ozone to the double bond to form a primary ozonide which decomposes to an excited bifunctional Criegee intermediate (12; 32). The intermediate can then isomerize, decompose or undergo collisions to form stabilized Criegee intermediates. The exact nature of the subsequent reactions of these stabilized Criegee intermediates is uncertain; Ziemann (18) summarizes them to include association reaction with acidic species, such as water, carboxylic acids and alcohols to form hydroperoxides, reactions with aldehydes and ketones to form secondary ozonides, and can undergo abstraction of oxygen atoms to form aldehydes or ketones. A significant fraction of the aerosols formed are dicarboxylic acids (12) although the reaction mechanism for the formation of these acids is uncertain (11).

Recent studies have identified oligomeric species in SOA (33). The standard model of SOA formation, based on gas-phase oxidation followed by gas-particle partitioning of oxidation products, does not explicitly account for heterogeneous chemistry occurring between absorbed molecules or between vapor molecules and particulate-phase species (3; 34-35). Recently it has been shown that a pre-existing acidic aerosol can catalyze additional SOA formation beyond that in the presence of more nearly neutral seed aerosol (36-40). The chemical mechanism(s) through which the additional SOA formation occurs

have not been confirmed, and whether an acidic aerosol substrate is required for formation of polymeric aerosol species has yet to be demonstrated.

In the present paper, we focus only on the overall SOA yields of the ozonolysis of the suite of cyclic alkenes. Our goal is to attempt to understand how SOA yield is related to certain essential structural features of the parent molecule, such as the number of carbon atoms, location of a double bond, and presence and location of methyl groups. Speciation of low molecular weight and oligomeric compounds in SOA from this class of parent hydrocarbons is addressed in a companion study (41).

7.3. Experimental Description

The ozonolysis experiments were carried out in the Caltech Indoor Chamber Facility, which has been described in detail elsewhere (6). In short, the facility is comprised of two heavily instrumented 28 m^3 suspended flexible Teflon chambers. The chamber material allows atmospheric pressure to be maintained at all times.

Particle size distribution and number concentrations were measured using two cylindrical scanning electrical mobility spectrometers (SEMS TSI model 3760), one dedicated to each chamber. Each SEMS uses a TSI model 3760 condensation particle counter (CPC) to count the number of particles selected by the SEMS. The sheath flow was set to 2.5 L min^{-1} and the inlet and classified aerosol flows were set to 0.25 L min^{-1}. The excess flow was allowed to balance the flows in the SEMS. Flows were calibrated using a bubble flow meter (Gilibrator, Gillian), and were continuously logged during experiments. Uncertainties in the flow were within 1%. Voltages were ramped between 30 and 700V allowing particle sizing from 25 to 700 nm diameter. Each scan was 237 s. Polystyrene latex spheres (Duke Scientific, Palo Alto, CA) were used to calibrate the size

selection of the SEMS. The average uncertainty of eight different PSL sizes used for calibration was 2%. Additional CPCs (TSI 3010 and TSI 3025) were used to monitor the total number concentration in each chamber and to identify episodes of nucleation. Agreement between the number concentrations determined by the SEMS and independent CPCs was 3%.

Temperature and RH within the chambers were measured using combined temperature and RH probes (Vaisala HMP230 series transmitters, Vaisala MA). The accuracy of the probe is 0.001 ˚C and 2% RH (when calibrated against salt solutions). The temperature of operation of the chambers was 20±1 ˚C and the RH was <10%. Over the course of an experiment temperature drift was generally within 1˚C, and RH drift was within 5%. The RH probes were calibrated with saturated salt solutions.

The concentration of the parent hydrocarbon was determined using a Hewlett-Packard 5890 Series gas chromatograph with a flame ionization detector (GC-FID) and a DB-5 60 m x 0.32 μm column (J&W Scientific, Davis CA). The GC response was calibrated for each parent hydrocarbon using a 50 L Teflon chamber. The uncertainty of the hydrocarbon concentration based on calibration errors was 2-5%. Ozone was measured using an ambient ozone monitor (Horiba APOA-360, Horiba, CA). The ozone monitor was calibrated using an internal ozone generator and nitrogen as zero air. The uncertainty of the ozone measurement was ±3%.

Between experiments, the chambers were continuously flushed with clean compressed air that had been passed through four scrubbing cartridges containing activated carbon, silica gel, purafil, and molecular-sieve, respectively, and a HEPA filter before entering the Teflon chambers. Flushing the chamber for 36 h before the start of an

experiment reduced the ozone and particle concentrations to below 1 ppb and 100 particles cm^{-3}, respectively.

In the experiments, $(NH_4)_2SO_4$ seed aerosol acted as a surface onto which the reaction products condensed. The initial volume of the aerosol was accurately known as the seed aerosol size distribution was intentionally prepared within the measurement size range of the SEMS. The presence of seed aerosol generally prevented homogeneous nucleation; this is important only insomuch as nucleation results in a significant number of particles with sizes below the smallest size measurable by the SEMS, precluding an accurate volume measurement. In addition, particle wall-loss rates could not be accurately quantified for those particles generated in a nucleation event. Data from experiments in which nucleation occurred were not included in this analysis.

Seed aerosol was generated using a stainless steel constant rate atomizer from a solution of 0.03 M $(NH_4)_2SO_4$ in ultra pure water. Dry aerosol was produced by passing the aerosol through a diffusion-dryer. Aerosol charge was reduced by mixing the aerosol stream with a neutralized air stream that had previously passed through two ^{210}Po neutralizers, and then by passing the aerosol stream through a Kr neutralizer before entering the chamber. Seed aerosol was atomized to a concentration of about 20,000 particles cm^{-3} and a mean diameter of 80-100 nm.

Cyclohexane was used as a scavenger to prevent oxidation of the cycloalkenes by OH, which is a well-established product of the alkene-ozone reaction (15). Recent studies (18, 42) have suggested that the identity of the OH scavenger influences SOA yield. For example, in the cycloalkene-ozone system, the use of propanol as the OH scavenger was found to lead to SOA products not found when cyclohexane as used as the OH scavenger,

while in the β-pinene-ozone system (42), cyclohexane scavenger resulted in greater SOA yield than when propanol was used. Cyclohexane was employed as a scavenger in the present study following the results presented in (18); a detailed discussion of the effect of the identity of SOA scavenger for these experiments will be presented elsewhere (43).

Cyclohexane was injected at sufficient concentration so that the reaction rate of OH radicals with the cyclohexane exceeded the reaction rate of the OH with the cycloalkene by a factor of 100.

Microliter syringes were used to inject known amounts of liquid hydrocarbons into the chambers. The compound was injected into a 250 ml glass bulb and gently heated as a stream of clean air was passed through the bulb, vaporizing the hydrocarbon and carrying it into the chamber. Cyclohexane was injected in the same way. Several measurements were made of the initial parent hydrocarbon concentrations, with the difference between three to 10 measurements being less than 1%.

The reaction was initiated with the beginning of ozone injection. Ozone was generated using a UV lamp ozone generator (EnMet Corporation, MI) and was injected into the chamber at 5 L min^{-1}. The total concentration of ozone injected was sufficient to exceed the parent hydrocarbon concentration by a factor of three.

Table 7.1 lists details of the parent hydrocarbons used, the cyclohexane scavenger, as well as the rate constants of the compounds for reaction with OH (k_{OH}) and ozone (k_{O3}).

7.4. Results and Discussion

7.4.1. SOA Yields

Seventy-five cycloalkene-ozonolysis experiments were performed on ten compounds (Table 7.2). The table lists the date of the experiment, the compound reacted, the

concentration of the compound consumed (ΔHC), and the mass concentration of SOA (ΔM_o) and the SOA yield (Y). ΔM_o was determined from the change in aerosol volume (measured by the SEMS) and assuming a particle density of 1.4 g cm^{-3}, as determined by Kalberer et al. (12) for the cyclohexene-ozone system. Measured particle number concentrations were corrected for size-dependent wall loss. The size-dependent wall loss for each chamber was determined experimentally by atomizing $(NH_4)_2SO_4$ aerosol into the chambers and measuring its decay over time. The first-order coefficient is maximum for particles less than 20 nm (0.01 particles min^{-1}), decreasing to a minimum loss rate of 0.0002 particles min^{-1} for particles of about 300 nm and increasing again for large particles (800 nm) to 0.001 particles min^{-1}. This behavior is consistent with that measured in other studies (44-45) and predicted by theory (46-47).

7.4.2. Yield and Carbon Number

Figure 7.2 shows the SOA yield curves for the basic cycloalkenes, cyclopentene, cyclohexene, cycloheptene, and cyclooctene. The error bars in Figure 7.2 (and all subsequent yield versus ΔM_o figures) are computed based on propagation of uncertainties arising in the ΔHC and ΔM_o measurements. For ΔHC, this includes propagation of the GC calibration uncertainties and the variance in the initial hydrocarbon measurements. For ΔM_o, this includes propagation of uncertainties in particle size (determined from calibration with polystyrene latex spheres) and differences in total particle number concentration determined by the independent CPC and SEMS.

The data in Figure 7.2 are fitted empirically with the two-product model of Equation 1, primarily as a convenient way to represent the data; the fitted coefficients (α_1, α_2, K_{om1} and K_{om2}) are listed in Table 7.3. The two-product yield curve is comprised of two parts.

At low $\Delta M_{o,}$ there is a rapid increase in yield, which most likely represents the partitioning of the lowest volatility products. In this section of the curve, both the partitioning coefficient and gas-phase stochiometry are important in determining the yield. The second part of the yield curve, which shows a reduction in the slope as a function of increasing $\Delta M_{o,}$ represents the partitioning of more volatile species as the aerosol organic volume increases; at high ΔM_o, the actual value of the species gas-particle partitioning coefficient becomes less important than the stochiometric mass yield.

Figure 7.2 shows that as carbon number inside the cycloalkene ring increases, SOA yield increases. In addition, two types of yield curves are displayed. For the low yield species, such as cyclopentene and cyclohexene, the curve flattens at high $\Delta M_{o,}$ while for high yield species, cycloheptene and cyclooctene, the yield curve shows no evidence of flattening. The fitted partition coefficients for the more volatile of the two empirical product species (K_{om2}) for the curve at high ΔM_o are very low for cycloheptene and cyclooctene (Table 7.3), suggesting that these products are quite volatile. Thus, for the high yield species cycloheptene and cyclooctene, the increasing yield as a function of ΔM_o is consistent with the presence of volatile species that are able to partition readily into the particle phase as ΔM_o increases, which may be due to continued gas-phase reactions or to the larger concentration of the volatile products. However, for the relatively low yielding compounds (cyclopentene and cyclohexene), the high volatility products (second of the two-product fit), in order to be able to partition into the particle phase, must have lower volatility as suggested by the larger K_{om2}, probably because they are not available in sufficiently large concentrations to allow partitioning at higher volatilities.

7.4.3. Yield and the Presence of a Methyl Group

Figures 7.3a-c compare the experimental yield data of each of the cycloalkenes with its analogous 1-methylated-cycloalkene. In each case the yield of the 1-methylated-cycloalkene exceeds that of the unmethylated homolog.

Figures 7.4a-c compare the experimental yield data for each of the cycloalkenes with the equivalent n-1 1-methylated-cycloalkene. As the total number of carbons in the compound increases, the SOA yield difference between the cycloalkene and equivalent n-1 cycloalkene increases. For cyclohexene and 1-methyl-1-cyclopentene, the yield curve for cyclohexene is slightly greater than that for 1-methyl-1-cyclopentene. However, for cycloheptene and 1-methyl-1-cyclohexene, the curves are similar until ΔM_o of 50 μg m^{-3}, then diverge with the slope of 1-methyl-1-cyclohexene being greater than for cycloheptene. 1-methyl-1-cycloheptene shows greater yield than cyclooctene for all ΔM_o.

Figure 7.5 compares the experimental yield curves for cyclohexene with its methylated homologues. As noted above, the presence of the methyl group on the double bonded carbon results in an increase in yield relative to the simple cycloalkene. However the presence of a methyl group at a site other than the double bond results in a dramatic decrease in SOA yield.

7.4.4. Yield and the Presence of an Exocyclic Double Bond

Also shown in Figure 7.5 is the experimental yield data for methylene cyclohexane. The methylene cyclohexane yield curve is slightly greater than the cyclohexene yield curve but is considerably lower than the 1-methyl-1-cyclohexene yield curve. The presence of an exocyclic double bond appears to offset the influence of the presence of a

methyl group so that, in effect, the yield for the compound with the n total carbons and an exocyclic double bond is similar to that of the n-1 cycloalkene.

7.4.5. Yield Curve for Terpinolene

The SOA yield curve for terpinolene was also determined in this study. Terpinolene has six carbons within its ring, an endocyclic and exocyclic double bond and a methyl group on the double bond (Figure 7.1). Based upon the above observations concerning the compounds studied here, we would expect the yield curve of terpinolene to lie above that of cyclohexene but below that of 1-methyl-1-cyclohexene. This is because the presence of the exocyclic double bond would tend to negate the positive (in yield terms) influence of the methyl group on the endocyclic double bond. Particularly, the exocyclic bond in terpinolene has greater degree of substitution than the endocyclic bond, and therefore greater reactivity (15), so that this bond is preferential for the initial ozone attack. Reaction of ozone with the remaining endocyclic double bond leads to products with a reduced number of carbon atoms and thus higher vapor pressure (26) resulting in reduced SOA yield.

The yield curve for terpinolene is shown in Figure 7.6, where it is compared with those of cyclohexene and 1-methyl-1-cyclohexene. Indeed, the yield curve for terpinolene lies qualitatively where one would expect it to be relative to the other two compounds.

7.4.6. Yield and Compound Structure: Multivariate Relationships

Is it possible to deduce the extent to which variable (carbon number, presence of an endocyclic or exocyclic double bond, presence of a methyl group on the double bond site, presence of a methyl group on a non-double bond site) has an effect on the yield? To

address this question, we performed a correlation analysis on a data set that included the yield at several ΔM_o values calculated from the two-product model fit, carbon number within the ring, exocyclic bond (represented by 1 if present or 0 if absent), endocyclic bond (represented by 1 if present or 0 if absent), location of methyl group on the double bond site (represented by 1 if present or 0 if absent), and location of methyl group on a non-double bond site (represented by 1 if present or 0 if absent).

Table 7.4 shows the correlation matrix resulting from simple linear correlation. While none of these variables displays exceptionally strong correlation, yield at various values of ΔM_o correlates most strongly with carbon number and the presence of a methyl group on the double bond, and is inversely correlated with the presence of a methyl group not on a double bond. Investigating the interrelationships of the variables further using principal component analysis reveals that 88% of the variance in the data set can be explained by three components (Table 7.5). The first component (58%) groups together variance in the yield at various values of ΔM_o, carbon number, and the presence of a methyl group on the double bond. The second component (explaining 17% of the variance) groups together the presence of both a methyl group and an exocyclic double bond. The third component, which explains only 13% of the variance, includes the presence of an endocyclic double bond.

7.4.7. Yield and Structure: Discussion

The structure of the precursor hydrocarbon has been found to affect the SOA yield. An increase in yield is observed with increase in carbon number within the cycloalkene ring. As noted above, the reaction between cyclohexene and ozone begins with the addition of ozone to the double bond to form a primary ozonide that decomposes to

produce an excited bifunctional Criegee intermediate (Figure 7.7). Kalberer et al. (12) showed the predominant aerosol species formed in the cyclohexene-ozone system were dicarboxylic acids (C_2, [oxalic], C_5 [glutaric] and C_6 [adipic]) and hydroxylated dicarboxylic acids (hydroxyglutaric acid hydroxyadipic acid). The hydroxylated dicarboxylic acids showed low overall molar yields; however, their low vapor pressures contributed significantly to total particle mass. For the larger cycloalkenes, cycloheptene and cyclooctene, predominant compounds in the aerosol phase are expected to be larger dicarboxylic acids (C_6 and C_7 [pimelic] for cycloheptene and C_7 and C_8 [suberic] for cyclooctene) and the analogous hydroxylated dicarboxylic acids. Ziemann (17) observed C_6 and C_7 dicarboxylic acids in the cycloheptene-ozone system and for the cyclodecene-ozone system the analogous dicarboxylic acids C_9 [sebacic] and C_{10} [zelaic] acids. These large dicarboxylic and hydroxylated dicarboxylic acids have low vapor pressure so that the mass of SOA produced by the oxidation of these cycloalkenes will be greater than that from the cycloalkenes with fewer carbons within the ring. Indeed, Gao et al. (41) also identified diacids and hydroxylated diacids as the main products in the low molecular weight species in these experiments, and reported a trend of increasing oligomer fraction with increasing carbon number. Details of the oligomer chemistry from these experiments are discussed in (41).

The presence of a methyl group located on the double bond site increases the SOA yield in each system. After the initial ozone addition to produce the primary ozonide, two Criegee intermediates are able to form due to the presence of the methyl group in the precursor compound (26) (Figure 7.7). These intermediates would lead to more abundant carbonyl acids than in the non-substituted cycloalkenes, and as a result more oligomers

may form from the 1-methyl-1-cycloalkene than from the cycloalkene. For example, Gao et al. (41) observed more C_7 carbonyl acids in the case of 1-methyl-1-cyclohexene, and suggested that this could favor the formation of C_{14} and larger dimers.

The presence of the methyl group on the non-double bonded carbon (3-methyl-1-cyclohexene), however, decreases SOA yield. While there are no published proposed mechanisms for the ozonolysis of 3-methyl-1-cyclohexene, the ozone attack and opening of the cycloalkene ring can be assumed to occur for this compound and as with 1-methyl-1-cyclohexene. Two Criegee intermediates form, this time with an additional methyl group located at the third carbon (Figure 7.7). One possible explanation lies in the polymer formation chemistry. Gao et al. (41) observed lower amounts of oligomers in the 3-methyl-cyclohexene oxidation products than in the 1-methyl-cyclohexene products. They speculated this to be partly due to a reduced likelihood of enol addition reactions occurring between the carbonyls and carbonyls acids produced from 3-methyl-cyclohexene than from 1-methyl-1-cyclohexene.

The effect of an exocyclic double bond is for SOA yield to be equivalent to the analogous n-1 cycloalkene. The reaction of ozone with methylene cyclohexane leads to an excited C_6 Criegee intermediate and formaldehdyde, or cyclohexanone and an excited C_1 Criegee intermediate (Figure 7.7) (24). Koch et al. (26) focused on the dicarboxylic acids produced during the ozonolysis of methylene cyclohexane and identified C_6 dicarboxylic acids as the predominant acids contributing to SOA. This is similar to the observations made for cyclohexene in (12) and (41); hence, similar yields observed for cyclohexene and methylene cyclohexene may be attributed to the similar products that form.

7.5. Acknowledgment

This research was supported by the Biological and Environmental Research Program (BER), U.S. Department of Energy, Grant No. DE-FG03-01ER 63099 and U.S. Environmental Protection Agency Grant RD-831-07501-0. Although the research described in this article has been funded in part by the U.S. Environmental Protection Agency, it has not been subjected to the Agency's required peer and policy review and therefore does not necessarily reflect the views of the Agency and no official endorsement should be inferred. Dr J. H. Kroll is thanked for helpful discussions.

7.6. References

(1) Turpin, B. J.; Huntzinger, J. J. *Atmos. Environ.* **1995***, 29,* 3527-3544.

(2) Janson, R.; Rosman, K.; Karlsson, A.; Hansson, H. C. *Tellus B.* **2001***, 53,* 423-440.

(3) Seinfeld, J. H.; Pankow, J. F. *Annual Rev. in Phys. Chem.* **2003,** *54,* 121-140.

(4) Lewis, A. C.; Carslaw, N.; Marriott, P. J.; Kinghorn, R. M.; Morrison, P.; Lee, A.; Bartle, K. D.; Pilling, M. J. *Nature,* **2001***, 405,* 778-781.

(5) Lamanna, M.; Goldstein, A. H. J. *Geophys. Res*. **1999**, *104,* 21247-21262.

(6) Cocker, D. R. III.; Flagan, R. C.; Seinfeld J. H. *Environ. Sci. Technol.* **2001,** *35*, 2594-2601.

(7) Odum, J. R.; Jungkamp, T. P. W; Griffin, R. J.; Flagan, R. C.; Seinfeld, J. H. *Science* **1997***, 276,* 96-99.

(8) Griffin, R. J; Cocker III, D. R; Flagan, R. C.; Seinfeld, J. H. *J. Geophys. Res.* **1999**, *104***,** 3555-3567.

(9) Pun, B. K.; Griffin, R. J.; Seigneur, C.; Seinfeld, J. H. *J. Geophys. Res.* **2002***, 107,* doi:10.1029/2001JD000542.

(10) Griffin, R. J.; Dabdub, D.; Seinfeld, J. H. *J. Geophys. Res.* **2002***, 107,* doi:10.1029/2001JD00541.

(11) Griffin, R. J.; Nguyen, K.; Dabdub, D.; Seinfeld, J. H. *J. Atmos. Chem.* **2003***, 44,* 171-190.

(12) Kalberer, M.; Yu, J.; Cocker, D. R.; Flagan, R. C.; Seinfeld, J. H. *Environ. Sci. Technol.* **2000**, *34,* 4894-4901.

(13) Hatakeyama, S.; Tanonaka, T.; Weng, J.; Bandow, H.; Takagi, H.; Akimoto, H. *Environ. Sci. Technol.* **1985,** *19,* 935-942.

(14) Izumi, K.; Murano, K.; Mizuochi, M.; Fukuyama, T. *Environ. Sci. Technol.* **1988,** *22,* 1207-1215.

(15) Atkinson, R. *J. Phys. Chem. Reference Data,* **1997,** *26,* 215-288.

(16) Gao, S.; Hegg, D. A.; Frick, G.; Caffrey, P. F.; Pasternack, L.; Cantrell, C.; Sullivan, W.; Ambrusko, J.; Albrechcinski, T.; Kirchstetter, T. W. *J. Geophys. Res.* **2001***, 106,* 27619-27634.

(17) Ziemann, P. J. *J. Phys. Chem. A,* **2002***, 106,* 4390-4402.

(18) Ziemann, P. J. *J. Phys. Chem. A,* **2003***, 107,* 2048-2060.

(19) Grosjean, E.; Grosjean, D.; Seinfeld, J. H. *Environ. Sci. Technol.* **1996,** *30,* 1038-1047.

(20) Grosjean, E.; Grosjean, D. *Int. J. Chem. Kin.* **1997,** *29,* 855-860.

(21) Hatakeyama, S.; Ohno, M.; Weng, J.-H.; Bandow, H.; Takagi, H.; Akimoto, H. *Environ. Sci. Technol.* **1987,** *21*, 52-57.

(22) Grosjean, E.; Grosjean, D. *Environ. Sci. Technol.* **1996,** *30,* 1321-1327.

(23) Atkinson, R.; Tuazon., E. C.; Aschmann, S. C. *Environ. Sci. Technol.* **1995,** *29,* 1860-1866.

(24) Hatakeyama, S.; Akimoto, H. *Bull. Chem. Soc. Jpn.* **1990,** *63,* 2701-2703.

(25) Grosjean, D.; Friedlander, S. K. Formation of organic aerosols from cyclic olefins and diolefins. In *The Character and Origins of Smog Aerosols*; Hidy, G. M., et al., Eds.; Wiley: New York, **1979***,* pp 435-473.

(26) Koch, S.; Winterhalter, R.; Uherek, E.; Kolloff, A.; Neeb, P.; Moortgat, G. K. *Atmos. Environ.* **2000***, 34,* 4031-4042.

(27) Hakola, H.; Arey, J.; Aschmann, S. M.; Atkinson, R. *J. Atmos. Chem.* **1994***, 18,* 75-102.

(28) Yu, J.; Flagan, R. C.; Seinfeld, J. H. *Environ. Sci. Technol.* **1998**, *32,* 2357-2370.

(29) Yu, J.; Jeffries, H. E.; Sexton, K. G. *Atmos. Environ.* **1997***, 31,* 2261-2280.

(30) Hallquist, M.; Wangberg, I.; Ljungstrom, E.; Barnes, I.; Becker, K. *Envrion. Sci.*

Tech. **1999***, 33,* 553-559.

(31) Hoffmann, T.; Bandaur, R.; Marggraf, U.; Linscheid, M. *J. Geophys. Res.* **1998***, 103,* 25569-25578.

(32) Atkinson, R.; Arey, J. *Chem. Rev. ASAP Web Release* **2003.**

(33) Limbeck, A.; Kulmala, M.; Puxbaum, H. *Geophys. Res. Lett.* **2003***, 19,* doi:10.1029/2003GL017738.

(34) Pankow, J. F.; Seinfeld, J. H.; Asher, W. E.; Erdakos, G. B. *Environ. Sci. Technol.* **2001***, 35,* 1164-1172.

(35) Seinfeld, J. H.; Erdakos, G. B.; Asher, W. E.; Pankow, J. F. *Environ. Sci. Technol.* **2001***, 35,* 1164-1172.

(36) Jang , M.; Czoschke, N. M.; Lee, S.; Kamens, R. M. *Science,* **2002***, 298,* 814-817.

(37) Jang, M..; Kamens, R. M. *Environ. Sci. Technol.* **2001***, 35,* 4758-4766.

(38) Czoschke, N. M; Jang, M.; Kamens, R. M. *Atmos. Environ.* **2003**, *37*, 4287-4299.

(39) Noziere, B.; Riemer, D. D. *Atmos. Environ.* **2003***, 37,* 841-851.

(40) Iinuma, Y.; Boge, O.; Gnauk, T.; Hermann, H. 2003, *Atmos*. *Environ.* **2004,** 38(5), 761-773.

(41) Gao, S.; Keywood, M. D.; Ng, N. L.; Surratt, J.; Varutbangkul, V.; Bahreini, R.; Flagan. R. C.; Seinfeld, J. H. **2003**, *J. Phys. Chem. A,* 10.1021/jp047466e.

(42) Docherty, K.S.; Ziemann, P. J. *Aerosol Sci. Tech.* **2004***, 37,* 877-891.

(43) Keywood, M. D.; Kroll, J. H.; Vartubangkul, V.; Bahreini, R.; Flagan, R. C.; Seinfeld, J. H. **2004,** *Environ. Sci. Technol.* 38 (12): 3343-3350.

(44) McMurry, P.; Grosjean, D. *Environ. Sci. Technol.* **1985,** *19,* 1176-1182.

(45) Park, S. H.; Kim, O. H.; Tan, Y. T.; Kown, S. B.; Lee, K. W. *Aerosol Sci. Tech.* **2001***, 35,* 710-717.

(46) Crump, J. G.; Seinfeld, J. H. *J. Aerosol Sci.* **1981***, 12,* 405-415.

(47) McMurry, P. H.; Rader, D. J. *Aerosol Sci. Tech.* **1985***, 4,* 249-268..

Table 7.1. Parent hydrocarbons

Compound	Formula	k_{OH} @ 298 K [1] (10^{-12} cm^3 molecule^{-1} s^{-1})	k_{O3} @ 298 K [2] (10^{-18} cm^3 molecule^{-1} s^{-1})	Supplier
Cyclopentene	C_5H_8	67	570	Aldrich Chemicals 96%
Cyclohexene	C_6H_{10}	67.7	81.4	Aldrich Chemicals 99+%
Cycloheptene	C_7H_{12}	74	245	Aldrich Chemicals 97%
Cyclooctene	C_8H_{14}	64	375	Aldrich Chemicals 96%
1-methyl-1-cyclopentene	C_6H_{10}	100	673	Aldrich Chemicals 97%
1-methyl-1-cyclohexene	C_7H_{12}	94	166	Aldrich Chemicals 97%
1-methyl-1-cycloheptene	C_8H_{14}	100	600 [4]	Chemsampco Inc, 98%
3-methyl-1-cyclohexene	C_7H_{12}	63	55 [4]	TCI America 95%
Methylene cyclohexane	C_7H_{12}	10	11	Aldrich Chemicals 98%
Terpinolene	$C_{10}H_{16}$	225	1880	Fluka 97%
Cyclohexane[3]	C_6H_{12}	7.2		Aldrich Chemicals, 99.9%

[1] Atkinson (15) except for 1-methyl-1-cyclopentene and 1-methy-1-1-cycloheptene, which were maximum estimates made from the k_{OH} of similar compounds, and cis-cyclooctene and 3-methyl-1-cyclohexene, which were estimated by Atkinson (personal communication, 2003). [2] Atkinson (15) except for methylene cyclohexane (20). [3] OH scavenger. [4] Estimated in the current study.

Table 7.2. Initial conditions and data for alkene ozonolysis experiments. A and B refer to the different chambers

Date		Parent	T (K)	ΔHC (ppb)	ΔM_o (μg m^{-3})	Y
04/21/03	A	Cyclopentene	293	192	57	0.105
04/23/03	A	Cyclopentene	293	141	30	0.074
04/25/03	A	Cyclopentene	293	105	22	0.073
04/28/03	A	Cyclopentene	293	224	57	0.091
06/02/03	A	Cyclopentene	293	154	37	0.086
06/09/03	A	Cyclopentene	293	117	24	0.073
06/16/03	A	Cyclopentene	293	86	12	0.051
09/02/03	A	Cyclopentene	294	254	73	0.102
10/02/03	A	Cyclopentene	293	173	38	0.078
01/27/03	B	Cyclohexene	292	206	111	0.158
01/29/03	B	Cyclohexene	294	240	101	0.141
02/06/03	B	Cyclohexene	292	119	45	0.111
02/08/03	B	Cyclohexene	292	59	14	0.072
02/10/03	B	Cyclohexene	292	173	81	0.136
03/03/03	B	Cyclohexene	292	81	25	0.090
06/04/03	B	Cyclohexene	292	313	200	0.187
02/04/03	A	Cycloheptene	292	212	202	0.238
02/12/03	A	Cycloheptene	293	158	131	0.208
02/14/03	A	Cycloheptene	293	100	66	0.166
02/16/03	A	Cycloheptene	293	48	19	0.101
02/19/03	A	Cycloheptene	293	282	289	0.257
03/01/03	A	Cycloheptene	293	66	39	0.148
03/24/03	A	Cycloheptene	292	184	168	0.228
09/12/03	A	Cycloheptene	293	110	88	0.375
09/30/03	A	Cycloheptene	292	186	146	0.201
04/11/03	B	Cyclooctene	292	195	248	0.277
04/14/03	B	Cyclooctene	292	142	165	0.236
04/16/03	B	Cyclooctene	292	98	97	0.215
04/18/03	B	Cyclooctene	292	57	43	0.166
05/09/03	B	Cyclooctene	293	24	13	0.118
05/12/03	B	Cyclooctene	293	169	223	0.289
07/02/03	B	Cyclooctene	293	277	536	0.423
04/21/03	B	1-methyl-1-cyclopentene	292	193	90	0.136
04/23/03	B	1-methyl-1-cyclopentene	293	145	49	0.099
04/25/03	B	1-methyl-1-cyclopentene	293	91	24	0.077
04/28/03	B	1-methyl-1-cyclopentene	292	70	13	0.055
04/30/03	B	1-methyl-1-cyclopentene	293	235	113	0.138
06/09/03	B	1-methyl-1-cyclopentene	292	163	73	0.130

Table 7.2. (continued)

Date		Parent	T (K)	ΔHC (ppb)	ΔM_o (μg m^{-3})	Y
01/27/03	A	1-methyl-1-cyclohexene	292	213	280	0.329
01/29/03	A	1-methyl-1-cyclohexene	294	205	261	0.320
02/06/03	A	1-methyl-1-cyclohexene	292	101	78	0.193
02/08/03	A	1-methyl-1-cyclohexene	293	51	26	0.126
02/10/03	A	1-methyl-1-cyclohexene	292	148	160	0.269
02/21/03	A	1-methyl-1-cyclohexene	292	254	417	0.410
03/03/03	A	1-methyl-1-cyclohexene	292	257	416	0.404
04/07/03	A	1-methyl-1-cyclohexene	293	157	136	0.218
10/06/03	A	1-methyl-1-cyclohexene	294	202	255	0.324
05/16/03	A	1-methyl-1-cycloheptene	293	96	152	0.346
05/16/03	B	1-methyl-1-cycloheptene	293	171	306	0.397
05/19/03	A	1-methyl-1-cycloheptene	294	70	91	0.287
05/19/03	B	1-methyl-1-cycloheptene	293	134	237	0.371
06/04/03	A	1-methyl-1-cycloheptene	292	49	53	0.238
06/06/03	B	1-methyl-1-cycloheptene	293	230	488	0.474
06/13/03	A	1-methyl-1-cycloheptene	293	21	18	0.191
10/08/03	B	1-methyl-1-cycloheptene	293	170	366	0.470
05/02/03	B	3-methyl-1-cyclohexene	292	219	66	0.076
05/05/03	A	3-methyl-1-cyclohexene	293	107	14	0.033
05/05/03	B	3-methyl-1-cyclohexene	292	151	35	0.057
05/07/03	A	3-methyl-1-cyclohexene	293	129	18	0.035
05/07/03	B	3-methyl-1-cyclohexene	292	307	120	0.097
06/02/03	A	3-methyl-1-cyclohexene	293	245	91	0.093
02/04/03	B	Methylene cyclohexane	293	218	145	0.178
02/12/03	B	Methylene cyclohexane	293	157	89	0.162
02/14/03	B	Methylene cyclohexane	292	102	32	0.097
02/16/03	B	Methylene cyclohexane	293	54	0	0.000
02/23/03	B	Methylene cyclohexane	292	341	237	0.190
04/07/03	B	Methylene cyclohexane	293	132	59	0.132
3/31/2003	A	Terpinolene	293	96.87	138	0.252
04/11/03	A	Terpinolene	293	188	289	0.271
04/14/03	A	Terpinolene	293	124	174	0.247
04/16/03	A	Terpinolene	293	98	121	0.219
04/18/03	A	Terpinolene	293	45	34	0.131
05/09/03	A	Terpinolene	293	20	6	0.048
05/14/03	A	Terpinolene	293	78	80	0.180
05/14/03	B	Terpinolene	292	237	373	0.277

Table 7.3. Aerosol yield parameters for the ozonolysis of cycloalkenes and related compounds (see Equation 1)

Parent	α_1	$K_{om,1}$ (m^3 μg^{-1})	α_2	$K_{om,2}$ (m^3 μg^{-1})
Cyclopentene	0.104	0.006	0.085	0.084
Cyclohexene	0.186	0.010	0.065	0.188
Cycloheptene	0.191	0.057	0.582	0.001
Cyclooctene	0.169	0.149	3.166	0.0002
1-methyl-1-cyclopentene	0.181	0.018	0.021	1.859
1-methyl-1-cyclohexene	0.138	0.164	0.954	0.001
1-methyl-1-cycloheptene	0.223	0.500	0.523	0.002
3-methyl-1-cyclohexene	0.067	0.035	0.085	0.009
Methylene cyclohexane	0.225	0.025	0.001	0.024
Terpinolene	0.312	0.012	0.043	0.641

Table 7.4. Matrix of correlation coefficients

	carbon number	endocyclic double bond	exocyclic double bond	methyl on double bond	methyl not on double bond
carbon number	1				
endocyclic double bond	0.076	1			
exocyclic double bond	-0.115	-0.667	1		
methyl on double bond	-0.187	0.272	0.102	1	
methyl not on double bond	-0.076	0.111	-0.167	-0.272	1
Y (ΔM_o =10 μg m^{-3})	**0.590**	0.223	-0.195	**0.467**	-0.360
Y (ΔM_o =100 μg m^{-3})	**0.598**	0.112	0.057	**0.546**	**-0.472**
Y (ΔM_o =200 μg m^{-3})	**0.599**	0.153	0.021	**0.566**	**-0.458**
Y (ΔM_o =300 μg m^{-3})	**0.619**	0.185	-0.036	**0.549**	**-0.440**
Y (ΔM_o =400 μg m^{-3})	**0.638**	0.206	-0.082	**0.523**	**-0.426**

Table 7.5. Results of principal component analysis

Component Matrix			
	Component		
	1	2	3
carbon number	**0.62**	0.13	**0.73**
endocyclic double bond	0.22	**0.85**	-0.31
exocyclic double bond	-0.06	**-0.91**	-0.02
methyl on double bond	**0.56**	-0.07	**-0.76**
methyl not on double bond	-0.48	0.41	0.22
Y (ΔM_o =10 μg m^{-3})	0.95	0.11	0.06
Y (ΔM_o =100 μg m^{-3})	**0.98**	-0.11	0.02
Y (ΔM_o =200 μg m^{-3})	**0.99**	-0.07	0.00
Y (ΔM_o =300 μg m^{-3})	**0.99**	-0.02	0.02
Y (ΔM_o =400 μg m^{-3})	**0.98**	0.02	0.05
Variance Explained	58%	17%	13%

Figure 7.1. Structure of parent hydrocarbons investigated in this study

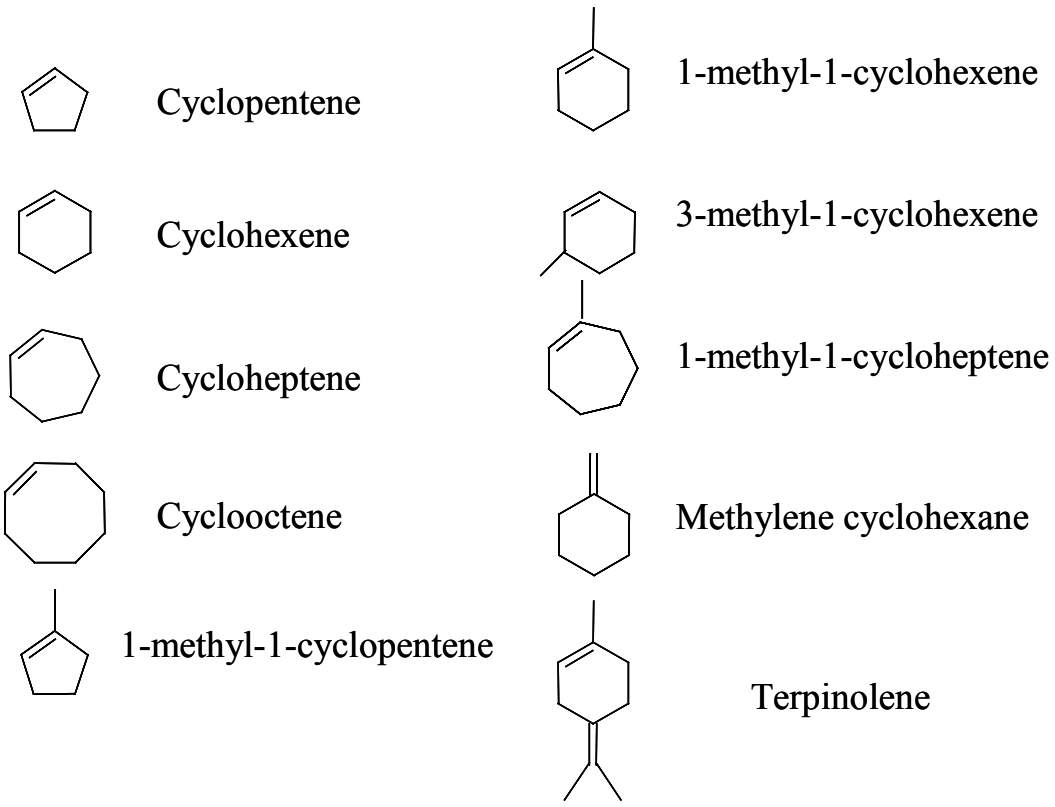

Figure 7.2. SOA yield data and curves fitted by Equation 1 as a function of ΔMo for the cycloalkenes

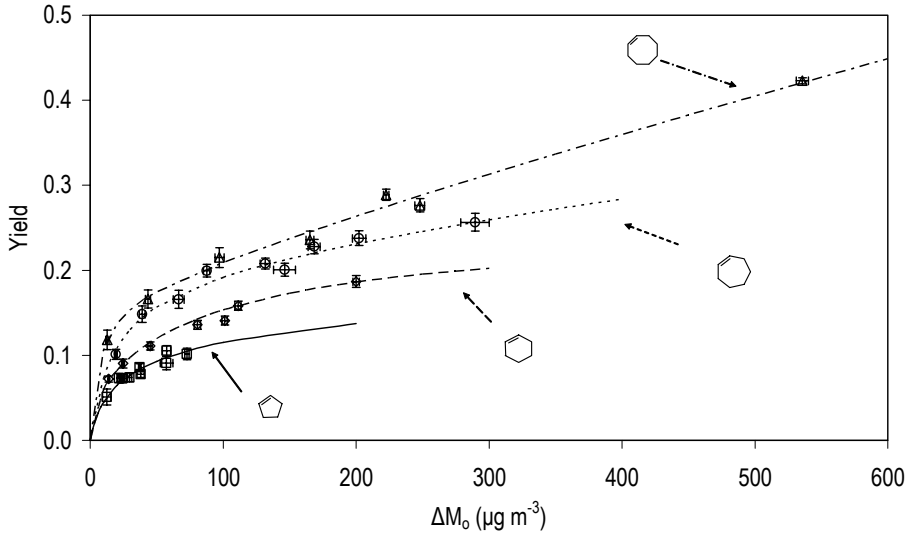

Figure 7.3. SOA yield data and curves fitted by Equation 1 as a function of ΔM_o for (a) cyclopentene and 1-methyl-1-cyclopentene, (b) cyclohexene and 1-methyl-1-cyclohexene, and (c) cycloheptene and 1-methyl-1-cycloheptene

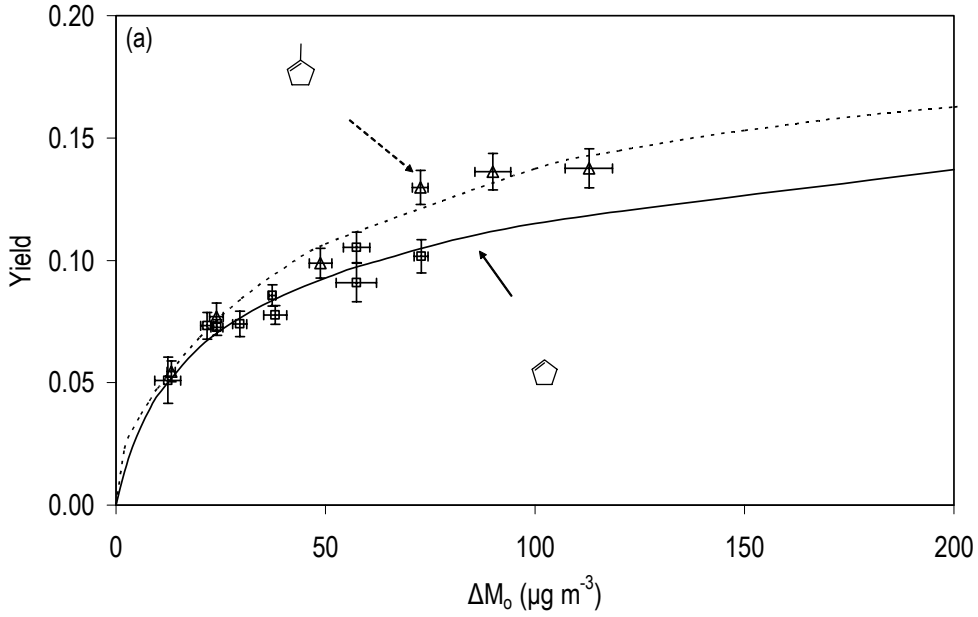

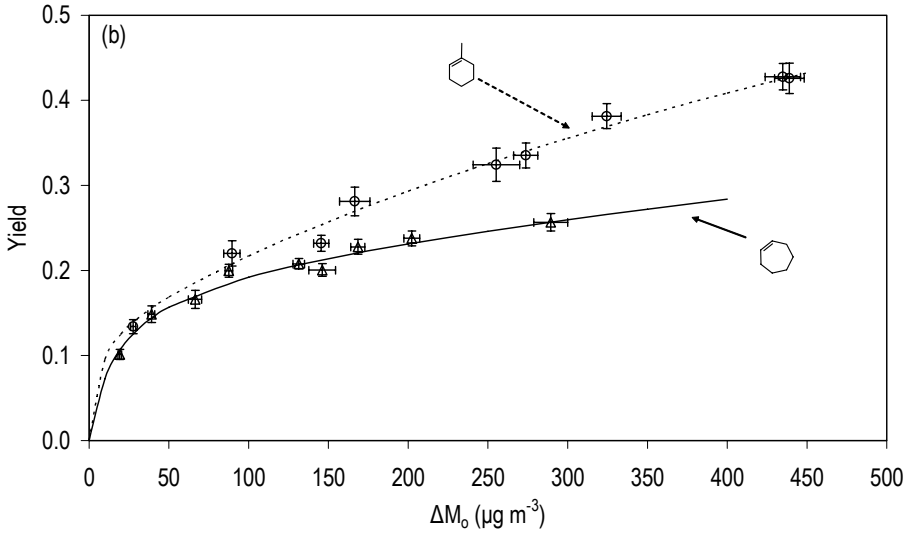

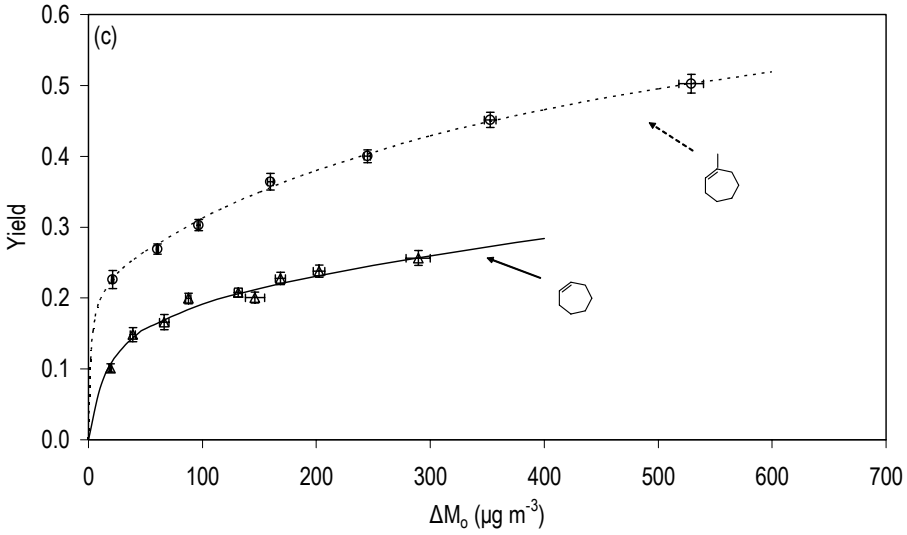
(c)
Yield
0.0
0.1
0.2
0.3
0.4
0.5
0.6
0
100
200
300
400
500
600
700
ΔM$_o$ (μg m^{-3})

Figure 7.4. Yield SOA yield data and curves fitted by Equation 1 as a function of ΔM_o for (a) cyclohexene and 1-methyl-1-cyclopentene, (b) cycloheptene and 1-methyl-1-cyclohexene and, (c) cyclooctene and 1-methyl-1-cycloheptene

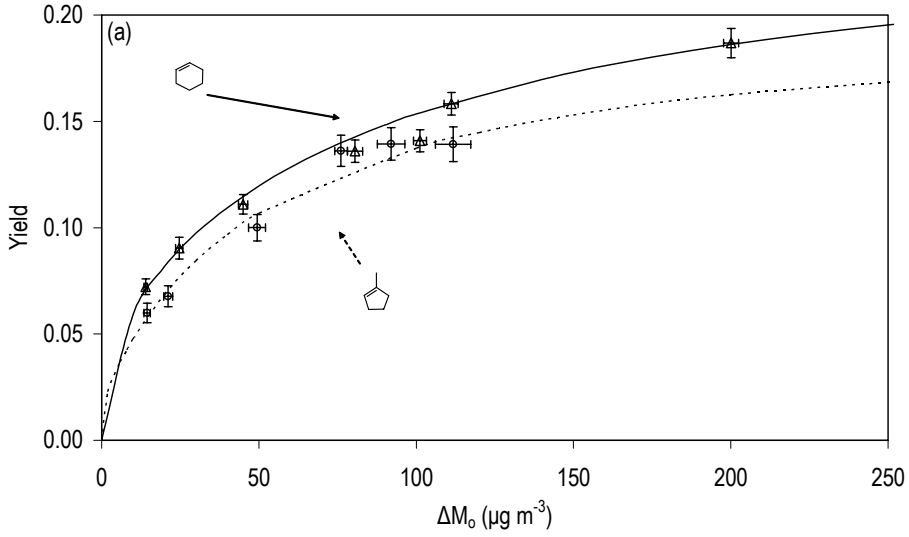

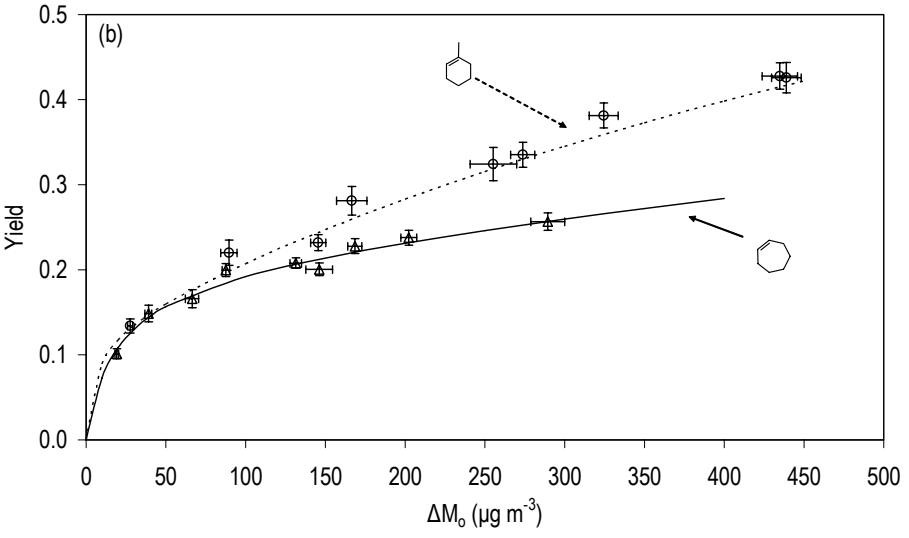

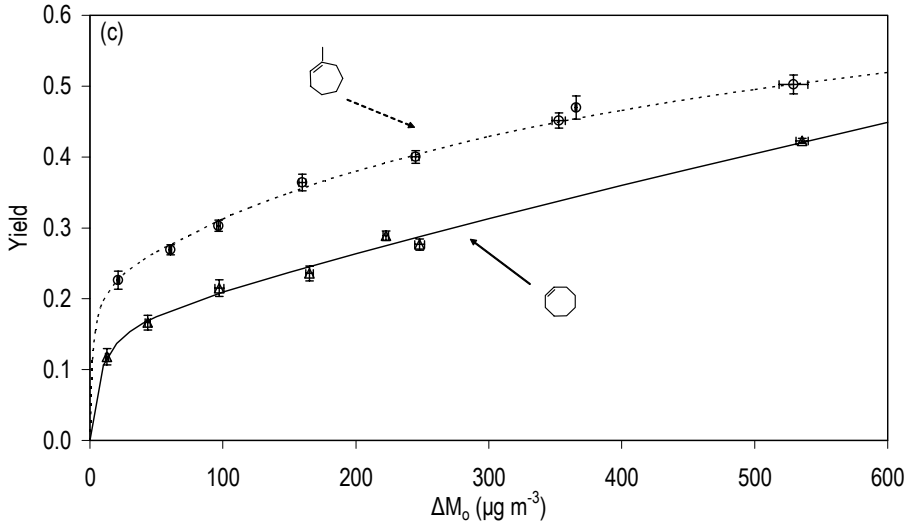
(c)
Yield
0.0
0.1
0.2
0.3
0.4
0.5
0.6
0
100
200
300
400
500
600
ΔM$_o$ (μg m^{-3})

Figure 7.5. SOA yield data and curves fitted by Equation 1 as a function of ΔM_o for for cyclohexene, 1-methyl-1-cyclohexene and 3-methyl-1-cyclohexene

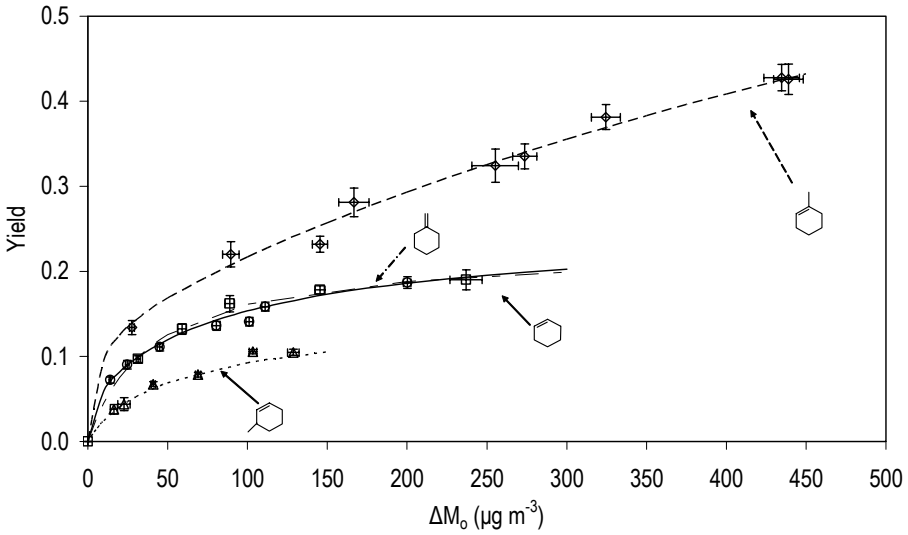

Figure 7.6. SOA yield data and curves fitted by Equation 1 as a function of ΔM_o for terpinolene relative to cyclohexene, 1-methyl-1-cyclohexene and methylene cyclohexane

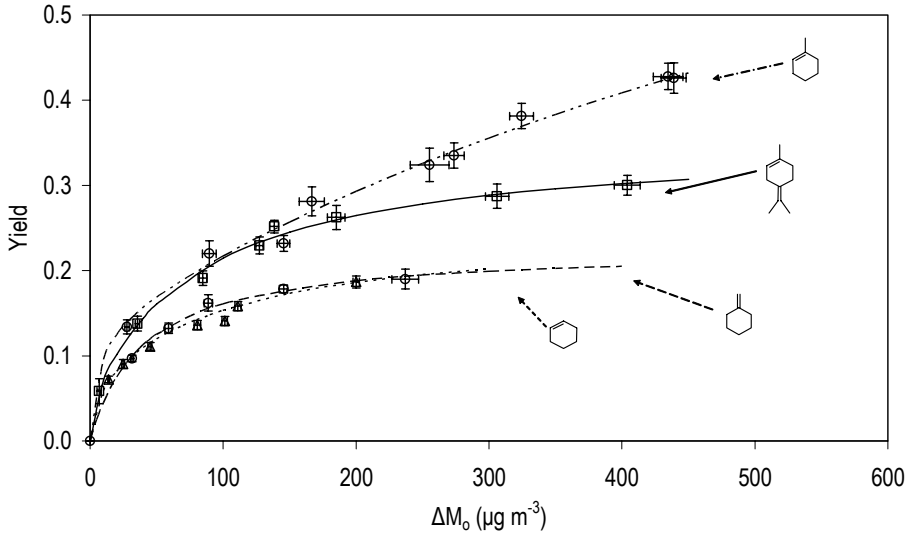

Figure 7.7. Initial ozone reactions with the main cycloalkene structures to form Criegee intermediates; A) cycloalkene; B) methyl group located on the double bond; C) methyl group not located on the double bond; D) endocyclic double bond